

Transport in defective quasi-one-dimensional arrays of chains of gold atoms on a vicinal silicon surface

Hiroyuki Okino, Iwao Matsuda, Shiro Yamazaki, Rei Hobara, and Shuji Hasegawa*

Department of Physics, School of Science, University of Tokyo, 7-3-1 Hongo, Bunkyo-ku, Tokyo 113-0033, Japan

(Received 16 February 2007; revised manuscript received 2 June 2007; published 20 July 2007)

The temperature dependence of electrical conductivity of quasi-one-dimensional arrays of metallic chains formed on a vicinal silicon surface, Si(553)-Au, was measured by a microscopic four-point probe method. A metal-insulator transition was observed around 160 K, which was expected from the previously observed charge density wave formation at low temperatures. This behavior was completely different from that of Si(557)-Au showing an insulating character only. Although both surfaces have similar atomic and electronic structures, differences in interchain coupling and defect density may explain the difference. Inevitably introduced point defects on the surfaces block conduction along the atomic chains. However, with enough interchain coupling, current can flow by avoiding the defects and moving to the adjacent chains on the Si(553)-Au, while it is almost prohibited on the Si(557)-Au due to smaller interchain coupling.

DOI: [10.1103/PhysRevB.76.035424](https://doi.org/10.1103/PhysRevB.76.035424)

PACS number(s): 73.25.+i, 68.35.Rh, 81.07.Vb

I. INTRODUCTION

One-dimensional (1D) systems have been extensively studied experimentally and theoretically to clarify their fundamental physics and to apply them to practical uses.^{1,2} Researchers attempt to realize the 1D (or quasi-1D) systems by using various kinds of materials, such as quantum wires, quantum edge states, nanowires (nanotubes), and highly anisotropic materials. Among them, anisotropic surface superstructures formed on semiconductor surfaces, which are the samples in this study, have some advantages. Although they adhere to the substrate, they are electronically isolated from the substrate crystal because the surface electronic states are located in the energy gap of the band structure of substrate bulk. Experimentally, the local atomic and electronic structures can be obtained in real space by scanning probe techniques,³ and electronic band dispersion can be obtained in k space by photoemission spectroscopy (PES).⁴ However, only a few transport properties of such surface superstructures are reported.⁵⁻⁸

We measured here transport properties of a highly anisotropic, therefore a quasi-1D, surface superstructure, Si(553)-Au,⁴ and compared the results with those of a similar surface, Si(557)-Au, reported in Ref. 5. Figure 1 shows scanning tunneling microscope (STM) images of the Si(553)-Au and Si(557)-Au. Both have arrays of atomic chains on narrow terraces of the vicinal surfaces, formed by depositing submonolayer (sub-ML) gold.⁹ The atomic chains are, however, interrupted by many point defects, which appear to be vacancies on the Si(553)-Au and bright protrusions on the Si(557)-Au, respectively. The structure and nature of these defects have not yet been identified. The protrusions on the Si(557)-Au resemble extra Si adatoms observed on Si(111)5×2-Au,¹⁰ which make the electronic state semiconducting locally.¹¹ The defects on the Si(553)-Au are also insulating locally, revealed by scanning tunneling spectroscopy (STS).¹² Nevertheless, quasi-1D metallic surface-state bands were detected by PES on both surfaces.^{4,13,14} They have two nearly half-filled and spin-split bands with large dispersion crossing the Fermi level (E_F).¹⁵ The Si(553)-Au has an ad-

ditional $\sim 1/3$ -filled band.^{4,13,16} The Fermi surfaces of the half-filled bands of both surfaces are nearly straight, indicating very small interchain coupling, whereas those of the $\sim 1/3$ -filled band are wiggling, indicating some interchain coupling.^{4,13,14,17} On the other hand, the 1D metal is in general unstable, which undergoes a metal-insulator (MI) transition upon cooling due to the Peierls instability.^{1,18} The MI transition is accompanied by lattice distortion as well as charge density wave (CDW) developing from the defects.³ Both of the Si(553)-Au and Si(557)-Au surfaces show the MI transition with successive band-gap opening in the multi-bands below room temperature (RT), as detected by PES^{16,19} and STS.^{3,20} As for electronic transport, we found here that the Si(553)-Au actually showed a MI transition, whereas the Si(557)-Au did not.⁵ Possible origin of this difference is discussed in terms of the inevitable point defects and interchain coupling.

II. EXPERIMENT

We used a P-doped n -type Si substrate having a resistivity of 1–10 Ω cm at RT, of which surface was inclined to the

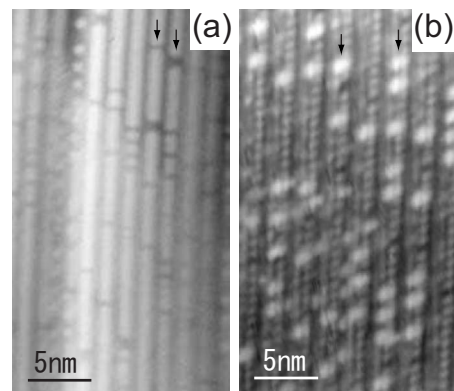


FIG. 1. STM images of the (a) Si(553)-Au and (b) Si(557)-Au surfaces. The tip biases were (a) 1.8 V and (b) -2.0 V, respectively. Some of the vacancies in (a) and protrusions in (b) are marked by arrows.

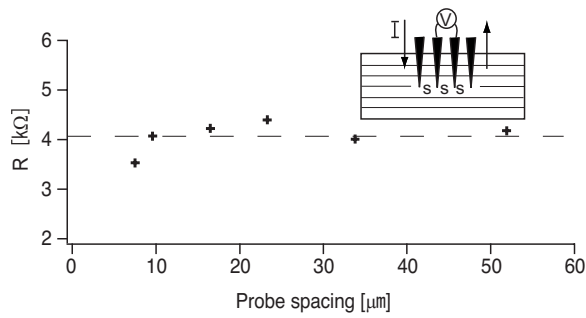


FIG. 2. Resistance of the Si(553)-Au as a function of probe spacing s in a linear M4PP method.

$[11\bar{2}]$ direction by 12.5° from (111). The Si(553)-Au surface was formed by depositing 0.24 ML of Au on the substrate held at 650°C , followed by annealing at 850°C . The surface is known to be composed of arrays of the atomic chains on regular narrow terraces, whose width is 1.48 nm separated by monatomic steps from each other.⁹ The Au coverage was calibrated using a phase diagram of Au/Si(111) superstructures.^{21,22}

The conductivity measurements were performed by microscopic four-point probe (M4PP) methods in micrometer regime with a four-probe STM and monolithic M4PP.^{23,24} Independently driven four W probes were used in the four-probe STM.²³ The probes contacted directly the sample surface during the 4PP measurements. A scanning electron microscope, integrated in the four-probe STM chamber, was used for observing the probe arrangement. The system operated at RT, and its base pressure was 3×10^{-10} Torr. The temperature (T) dependence of conductivity from 270 to 120 K was measured using a variable-temperature M4PP system.²⁴ This system used a commercial monolithic 4PP of 20 μm probe spacing.²⁵ The probe was cooled down to the same temperature as the sample and made a direct contact with the sample surface. The base pressure was 1×10^{-10} Torr.

Usually, the measured 4PP conductivity involves contributions from the surface states, the surface space-charge layer, and the substrate bulk.²⁶ In the M4PP method, the interprobe distance is reduced to micrometer scale to enhance the surface sensitivity, because in this case the electrical current flows mainly near the surface region. Then, this method is shown to be effective for measuring the surface-state conductivity.⁶ The surface-state conductivity corresponds to the conductivity of the arrays of the atomic chains here. We confirmed that we really detected the surface-state conductivity by measuring the anisotropy in conductivity²⁷ and probe-spacing dependence, as will be shown below.

The dimensionality of electrical conduction was investigated using the four-probe STM²³ by changing the probe spacing in the linear M4PP method. In the linear M4PP measurements, in which four probes are aligned on a line with equidistance, the electrical current (I) flows through the outer pair of probes, and the voltage drop (V) between the inner pair of probes is measured, as shown by an inset in Fig. 2. Thus, I - V curves were taken, giving a resistance $R=dV/dI$. The resistance R , on the other hand, can be calculated from

Poisson's equation by assuming homogenous conductors.²⁸ When the current flows through a thin sheet in two-dimensional (2D) way, R is independent of the probe spacing s . When the current flows in 1D way (through a thin wire) or in three-dimensional (3D) way (through a bulky sample), R is dependent on the probe spacing; $R \propto s$ for 1D and $R \propto 1/s$ for 3D. Thus, we can know the dimensionality of electrical conduction by investigating the probe-spacing dependence. The 2D conduction is realized when the penetration depth of the electrical current is small enough compared with the probe spacing even when the sample is bulky.

III. RESULTS

First, we investigated the dimensionality of electrical conduction on the Si(553)-Au using the four-probe STM at RT. The four probes were aligned on a line parallel to the atomic-chain direction. The measured resistance R is plotted in Fig. 2 as a function of the probe spacing s . The R is independent of the probe spacing. This means that the electrical current flows in 2D way on the Si(553)-Au by spreading out laterally across the atomic chains on the surface and does not flow into the substrate bulk in 3D way. Due to band bending, as will be mentioned later, the electrical current is confined near the surface region by a pn junction between the subsurface region (surface space-charge layer) and the underlying bulk region. This is a benefit of using the n -type wafer: an inversion layer is formed beneath the surface. Therefore, the measured conductivity is a sum of the surface-state conductivity and the space-charge-layer conductivity only. In spite of the 1D character of the Si(553)-Au, the electrical current flows not only along the atomic chains but also spreads laterally due to interchain coupling and/or the isotropic space-charge layer beneath the surface.

The space-charge-layer conductivity can be estimated from the density of free carriers and mobility there.²⁹ The carrier density is calculated from the density of states of Si and the Fermi-Dirac distribution function once we know the position of band edge with respect to E_F .²⁶ The bulk-valence-band maximum at the surface is located at ~ 0.25 eV below E_F ,⁴ which means a light inversion layer on the n -type substrate. Assuming that the doping concentration in the Si crystal is uniform up to the surface, the space-charge-layer conductivity was calculated to be $\sim 1 \mu\text{S}/\square$. Because the space-charge-layer mobility is unknown, we have used the bulk value of mobility in the above calculation, which is usually higher than the space-charge-layer mobility. The above value thus gives an upper limit of the space-charge-layer conductivity. Therefore, it is negligible compared with the measured conductivity ($\sim 100 \mu\text{S}/\square$). If the doping concentration in the Si crystal is not uniform due to high-temperature heating for cleaning the surface, the p -type region at the subsurface can be thicker than the uniform case as pointed out by Tung *et al.*³⁰ This is caused by the boron contamination incorporated into the subsurface region in the Si crystal. Thus, if we assume the p -type region to extend 500 nm in depth, the space-charge-layer conductivity is estimated to be $\sim 15 \mu\text{S}/\square$, which is still much smaller than the measured conductivity ($\sim 100 \mu\text{S}/\square$). Thus, we can say that the main

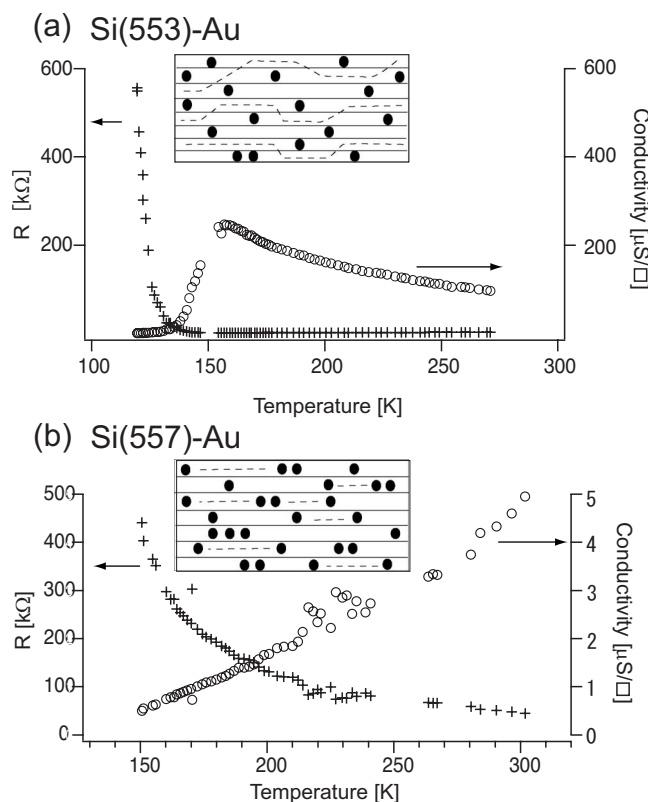


FIG. 3. Temperature dependence of the conductivity (circle) and resistance (cross) of the (a) Si(553)-Au and (b) Si(557)-Au. Insets are schematic drawings of carrier transport around RT, where dots represent point defects and broken lines represent conduction paths.

contribution to the measured conductivity is the surface-state conductivity for the Si(553)-Au.

Next, T dependence of the surface-state conductivity of the Si(553)-Au was measured, as shown in Fig. 3(a). The conductivity increased with cooling down to around 160 K, showing a metallic character, while it began to decrease drastically by further cooling. Thus, a MI transition occurred around 160 K. As mentioned before, the MI transition was also observed in PES¹⁶ and STS³ by showing an energy gap opening by cooling. It seems, however, that the transition temperature is different among the experiments: a band gap opens already at 250 K in PES,¹⁶ while a metallic I - V curve still remains even at 110 K in STS.³ Both seem inconsistent with our transition temperature in transport measurement.

On the other hand, as shown in Fig. 3(b), the Si(557)-Au shows a T dependence of conductivity which is completely different from that of Si(553)-Au. This activation-type insulating T dependence⁵ is inconsistent with a MI transition in the electronic structure observed by PES and STS for the Si(557)-Au.^{19,20}

We note that the MI transition in conductivity of the Si(553)-Au shows a single band-gap opening, while the MI transition in PES¹⁶ and STS³ represented successive band-gap openings of the three surface-state bands. This discrepancy indicates that only one band ($\sim 1/3$ -filled band) contributes to the conductivity change, which will be discussed later.

IV. DISCUSSION

Now, we are faced with two questions. First, the MI-transition temperature of the Si(553)-Au is different among the experimental methods, PES (~ 250 K),¹⁶ STS (below 110 K),³ and transport (~ 160 K). Second, the T dependence of the conductivity is completely different between the Si(553)-Au and the Si(557)-Au,⁵ although the T dependence of the PES¹⁶ and STS³ of the Si(553)-Au is similar to those of the Si(557)-Au.^{19,20}

The difference in the MI-transition temperature among experimental methods is attributed to the difference in the nature of experimental methods themselves and/or the difference in the defect density on samples. On the Si(553)-Au surface, the CDW nucleates around the defects and spreads along the atomic chains with decreasing temperature.³ In conductivity measurements, the MI transition occurs when insulating CDW regions develop sufficiently and metallic percolation paths are cut by the insulating regions. This means that the MI transition can occur even if the whole surface is not insulating. In contrast, the MI transition in the STS measurement³ is observed when the whole surface becomes insulating because the STS spectra in Ref. 3 were spatially averaged. On the other hand, the MI transition in the PES measurement¹⁶ occurs when the insulating regions start developing, because the band-gap opening was defined by the energy shift of a leading edge in PES spectra. Thus, by assuming such an inhomogeneous mixture of metallic and insulating regions during the MI transition at intermediate temperatures, it is reasonable to think that the STS showed a metallic behavior and the PES showed a band-gap opening around 160 K at which the conductivity exhibited the MI transition.

Another possible reason for the apparently different MI-transition temperatures among the experimental methods is that the defect density on the samples might be different in different research groups. From our experience, the density of point defects such as dark vacancies [Fig. 1(a)] and bright protrusions [Fig. 1(b)] can differ even if the sample preparation procedure is almost the same.³¹ The defect density sensitively depends on the annealing procedure during sample preparation.³² Since the MI transition is a defect-mediated CDW transition,³ it is natural that the transition temperature is higher when the defect density is higher.

The T dependence of the surface-state conductivity of the Si(557)-Au is shown in Fig. 3(b), which is already reported in our previous paper.⁵ Although the Si(553)-Au and the Si(557)-Au have similar Au/Si compositions and atomic and/or band structures, the behaviors of conductivity are completely different. The conductivity of Si(557)-Au shows an activation-type insulating behavior from RT to 150 K, whereas that of Si(553)-Au is metallic above 160 K. Since PES as well as STS indicate both surfaces to be metallic at RT,^{3,16,19,20} the T dependence of conductivity for the Si(553)-Au around RT is consistent with the results of PES and STS, while inconsistent for the Si(557)-Au.

This difference is considered to come from differences in the defect density and the band structure. A lot of point defects, as shown in Fig. 1, are intrinsically introduced on both of the Si(553)-Au and the Si(557)-Au surfaces and cannot be

removed completely though the density can be changed by annealing. The defect density on the Si(553)-Au is usually lower than that on the Si(557)-Au.⁴ Both surfaces have two nearly degenerate half-filled surface-state bands, which have almost no dispersion perpendicular to the chains.^{4,13,14,17} However, only the Si(553)-Au has the additional $\sim 1/3$ -filled band, which has weak dispersion perpendicular to the atomic chains.^{4,13} Thus, only the carriers of the $\sim 1/3$ -filled band of the Si(553)-Au have the velocity component across the chains. Indeed, we measured the conductivity perpendicular to the chains to be $30 \mu\text{S}/\square$ for the Si(553)-Au,³³ while only $3.5 \mu\text{S}/\square$ for the Si(557)-Au.⁵

Previous STS measurements showed finite density of states at E_F on the defect-free region, while a clear energy gap opening on the defects as well as on the chain ends was terminated by the defects on Si(553)-Au.¹² Thus, the metallic chains are divided into metallic segments by the insulating defects. Carriers are then scattered by the defects. Although the nature of carrier scattering by the protrusions on the Si(557)-Au may be different from that by the vacancies on the Si(553)-Au, we can estimate that the carriers are more strongly scattered on the Si(557)-Au by the following reason. As will be reported elsewhere, by using the square-four-point probe method, we measured the conductivity along the Au chains on both of the Si(553)-Au and Si(557)-Au and revealed that the conductivity on the Si(557)-Au ($\sim 9 \mu\text{S}/\square$) was much lower than that on the Si(553)-Au ($\sim 80 \mu\text{S}/\square$). This suggests that the protrusions on the Si(557)-Au more effectively interrupt the electrical conduction along the Au chains.³³ Thus, on the Si(557)-Au, the defect density is so high and the band dispersion perpendicular to the chain is so small that there is no percolating metallic path even at RT. Thus, a nearest-neighbor-hopping-type conduction takes

place on the Si(557)-Au.⁵ On the other hand, on the Si(553)-Au, the defect density is lower than that on the Si(557)-Au, and carriers in the $\sim 1/3$ -filled band can move across the chains. Thus, carriers can avoid the defects on the chains by moving to the neighboring chains, as schematically illustrated by the inset in Fig. 3(a). Therefore, the conductivity of Si(553)-Au shows a metallic behavior around RT. The MI transition observed in the conductivity of Si(553)-Au is electronically originated due to the Peierls instability as reported in PES and STS measurements.^{3,16} Because the half-filled bands of the Si(553)-Au do not contribute to the conductivity due to little dispersion across the chains, the T dependence of conductivity shows a single-band MI transition due to the $\sim 1/3$ -filled band only.

V. SUMMARY

We have measured the T dependence of conductivity of the arrays of the atomic chains of the quasi-1D Si(553)-Au. The MI transition is found to occur around 160 K, which is qualitatively consistent with the previous PES and STS results. By comparing the results with those of the Si(557)-Au, we have shown that atomic-scale point defects and inter-chain coupling decisively govern the nature of transport in quasi-1D systems. Thus, nano-scale information about atomic and/or electronic structures is essential to evaluate macroscopically averaged properties such as conductivity.

ACKNOWLEDGMENTS

This work has been supported by Grants-In-Aid and A3 Foresight Program from Japanese Society for the Promotion of Science.

*Corresponding author; shuji@surface.phys.s.u-tokyo.ac.jp

¹G. Grüner, *Density Waves in Solids* (Addison-Wesley, Reading, MA, 1994).

²C. M. Lieber, *MRS Bull.* **28**, 486 (2003).

³P. C. Snijders, S. Rogge, and H. H. Weitering, *Phys. Rev. Lett.* **96**, 076801 (2006).

⁴J. N. Crain, J. L. McChesney, F. Zheng, M. C. Gallagher, P. C. Snijders, M. Bissen, C. Gundelach, S. C. Erwin, and F. J. Himpsel, *Phys. Rev. B* **69**, 125401 (2004).

⁵H. Okino, R. Hobara, I. Matsuda, T. Kanagawa, S. Hasegawa, J. Okabayashi, S. Toyoda, M. Oshima, and K. Ono, *Phys. Rev. B* **70**, 113404 (2004).

⁶T. Tanikawa, I. Matsuda, T. Kanagawa, and S. Hasegawa, *Phys. Rev. Lett.* **93**, 016801 (2004).

⁷T. Kanagawa, R. Hobara, I. Matsuda, T. Tanikawa, A. Natori, and S. Hasegawa, *Phys. Rev. Lett.* **91**, 036805 (2003).

⁸C. Tegenkamp, Z. Kallassy, H. Pfnür, H.-L. Günter, V. Zielasek, and M. Henzler, *Phys. Rev. Lett.* **95**, 176804 (2005).

⁹J. N. Crain and F. J. Himpsel, *Appl. Phys. A: Mater. Sci. Process.* **82**, 431 (2006).

¹⁰R. Bennowitz, J. N. Crain, A. Kirakosian, J.-L. Lin, J. L. McChesney, D. Y. Petrovykh, and F. J. Himpsel, *Nanotechnology*

13, 499 (2002).

¹¹H. S. Yoon, S. J. Park, J. E. Lee, C. N. Whang, and I.-W. Lyo, *Phys. Rev. Lett.* **92**, 096801 (2004).

¹²J. N. Crain and D. T. Pierce, *Science* **307**, 703 (2005).

¹³J. N. Crain, A. Kirakosian, K. N. Altmann, C. Bromberger, S. C. Erwin, J. L. McChesney, J. L. Lin, and F. J. Himpsel, *Phys. Rev. Lett.* **90**, 176805 (2003).

¹⁴R. Losio, K. N. Altmann, A. Kirakosian, J. L. Lin, D. Y. Petrovykh, and F. J. Himpsel, *Phys. Rev. Lett.* **86**, 4632 (2001).

¹⁵I. Barke, F. Zheng, T. K. Rugheimer, and F. J. Himpsel, *Phys. Rev. Lett.* **97**, 226405 (2006).

¹⁶J. R. Ahn, P. G. Kang, K. D. Ryang, and H. W. Yeom, *Phys. Rev. Lett.* **95**, 196402 (2005).

¹⁷P. Segovia, D. Purdie, M. Hengsberger, and Y. Baer, *Nature (London)* **402**, 504 (1999).

¹⁸H. W. Yeom, S. Takeda, E. Rotenberg, I. Matsuda, K. Horikoshi, J. Schaefer, C. M. Lee, S. D. Kevan, T. Ohta, T. Nagao, and S. Hasegawa, *Phys. Rev. Lett.* **82**, 4898 (1999).

¹⁹J. R. Ahn, H. W. Yeom, H. S. Yoon, and I. W. Lyo, *Phys. Rev. Lett.* **91**, 196403 (2003).

²⁰H. W. Yeom, J. R. Ahn, H. S. Yoon, I. W. Lyo, H. Jeong, and S. Jeong, *Phys. Rev. B* **72**, 035323 (2005).

- ²¹R. Plass and L. D. Marks, *Surf. Sci.* **380**, 497 (1997).
- ²²T. Nagao, S. Hasegawa, K. Tsuchie, S. Ino, C. Voges, G. Klos, H. Pfnur, and M. Henzler, *Phys. Rev. B* **57**, 10100 (1998).
- ²³I. Shiraki, F. Tanabe, R. Hobara, T. Nagao, and S. Hasegawa, *Surf. Sci.* **493**, 633 (2001); S. Hasegawa, I. Shiraki, F. Tanabe, and R. Hobara, *Curr. Appl. Phys.* **2**, 465 (2002).
- ²⁴T. Tanikawa, I. Matsuda, R. Hobara, and S. Hasegawa, *e-J. Surf. Sci. Nanotechnol.* **1**, 50 (2003).
- ²⁵See Capres, <http://www.capres.com/>
- ²⁶S. Hasegawa, X. Tong, S. Takeda, N. Sato, and T. Nagao, *Prog. Surf. Sci.* **60**, 89 (1999).
- ²⁷The anisotropy (a ratio between the conductivity along the chain arrays and that in the perpendicular direction) was 2.7, which was much smaller than the value calculated from the anisotropic band dispersion and Fermi surface using the Boltzmann equation. Details will be reported elsewhere.
- ²⁸J. D. Wasscher, *Philips Res. Rep.* **16**, 301 (1961).
- ²⁹H. Lüth, *Surfaces and Interfaces of Solid Materials* (Springer-Verlag, Berlin, 1995).
- ³⁰R. T. Tung, K. K. Ng, J. M. Gibson, and A. F. J. Levi, *Phys. Rev. B* **33**, 7077 (1986).
- ³¹H. Okino, I. Matsuda, T. Tanikawa, and S. Hasegawa, *e-J. Surf. Sci. Nanotechnol.* **1**, 84 (2003).
- ³²J. N. Crain, M. D. Stiles, J. A. Stroscio, and D. T. Pierce, *Phys. Rev. Lett.* **96**, 156801 (2006).
- ³³The data of anisotropic conductivity will be reported elsewhere.